

Enhanced Exopolymer Production and Chromium Stabilization in *Pseudomonas putida* Unsaturated Biofilms

John H. Priestler,¹ Scott G. Olson,¹ Samuel M. Webb,² Mary P. Neu,³ Larry E. Hersman,⁴
and Patricia A. Holden^{1*}

Donald Bren School of Environmental Science & Management, University of California, Santa Barbara, California 93106-5131¹;
Stanford Synchrotron Radiation Laboratory, Stanford Linear Accelerator Center, Menlo Park, California 94025²;
Chemistry Division, Los Alamos National Laboratory, Los Alamos, New Mexico 87545³; and
Bioscience Division, Los Alamos, National Laboratory, Los Alamos, New Mexico 87545⁴

Received 19 August 2005/Accepted 15 December 2005

Chromium-contaminated soils threaten surface and groundwater quality at many industrial sites. In vadose zones, indigenous bacteria can reduce Cr(VI) to Cr(III), but the subsequent fate of Cr(III) and the roles of bacterial biofilms are relatively unknown. To investigate, we cultured *Pseudomonas putida*, a model organism for vadose zone bioremediation, as unsaturated biofilms on membranes overlaying iron-deficient solid media either containing molecular dichromate from potassium dichromate (Cr-only treatment) or with deposits of solid, dichromate-coated hematite (Fe+Cr treatment) to simulate vadose zone conditions. Controls included iron-deficient solid medium and an Fe-only treatment using solid hematite deposits. Under iron-deficient conditions, chromium exposure resulted in lower cell yield and lower amounts of cellular protein and carbohydrate, but providing iron in the form of hematite overcame these toxic effects of Cr. For the Cr and Fe+Cr treatments, Cr(VI) was completely reduced to Cr(III) that accumulated on biofilm cells and extracellular polymeric substances (EPSs). Chromium exposure resulted in elevated extracellular carbohydrates, protein, DNA, and EPS sugars that were relatively enriched in *N*-acetyl-glucosamine, rhamnose, glucose, and mannose. The proportions of EPS protein and carbohydrate relative to intracellular pools suggested Cr toxicity-mediated cell lysis as the origin. However, DNA accumulated extracellularly in amounts far greater than expected from cell lysis, and Cr was liberated when extracted EPS was treated with DNase. These results demonstrate that Cr accumulation in unsaturated biofilms occurs with enzymatic reduction of Cr(VI), cellular lysis, cellular association, and extracellular DNA binding of Cr(III), which altogether can facilitate localized biotic stabilization of Cr in contaminated vadose zones.

Chromium (Cr), an Environmental Protection Agency priority pollutant and suspected carcinogen (16), is a significant soil contaminant at many industrial sites, where it is used for manufacturing alloys and pigments, electroplating, leather tanning, wood preservation, and chemical synthesis (43). Chromium is also an important soil and water contaminant at several U.S. Department of Energy facilities (37, 68). The prevalent oxidation states of chromium in the soil environment are VI and III (38). Cr(VI) is toxic and poses a public health risk because of its mobility and the ease with which it can enter eukaryotic cells (10). The reduced state, Cr(III), however, is less soluble and is regarded as relatively harmless to humans. Thus, remediation efforts often focus on reduction-mediated immobilization of Cr (12).

Bacteria are often involved in the fate and transport of toxic metals in soil (35, 36, 50, 62). Both abiotic and biotic processes catalyze the reduction of Cr(VI) to Cr(III) in the natural environment (20), but bacterial reduction of Cr(VI) to Cr(III) can occur under nutrient-amended vadose zone conditions, which implies that biostabilization is a viable management option (42). In laboratory studies, Cr(VI) is actively transported into cells and then intracellularly reduced and effluxed as Cr(III) via the ChrA system (1). In *Pseudomonas* spp., Cr(III) then

accumulates on the cell wall and outer membrane (63). Similar processes have been documented for other bacterial species and toxic metals (2, 29, 41, 60, 66). However, bacterium-metal interactions in the environment will also involve extracellular polymeric substances (EPSs) of bacterial biofilms, the form of bacterial growth most frequently occurring in nature (13, 14).

EPS facilitates nutrient and water retention, cell/substrate adhesion, cell-cell signaling, and protection of individual cells from chemical degradation or attack (5, 56, 57). Bacterial EPS can also bind contaminants (9, 59, 67, 72), which can lead to short-term stabilization or longer-term immobilization of metals (9). Metals also bind to cells in biofilms, as indicated by *Pseudomonas aeruginosa* biofilm cells accumulating relatively more Fe, Au, and La than planktonic *P. aeruginosa* (34). Cr(VI) binds to biofilms (11), but little is known about its specific interactions with either EPS or biofilm cells. Inferences can be drawn from *Enterobacter cloacae* grown in seawater, whereby Cr(VI) exposure resulted in increased EPS production and metal binding to cells and EPS (31). However, interactions of EPS and Cr may depend on the abundance and chemistry of EPS, which in turn varies with bacterial strain and nutrition.

EPS is composed of carbohydrates, protein, DNA, and sorbed abiotic constituents (56). Changes in the macromolecular composition of bacterial biofilms have been observed with alterations in carbon source (55), water availability (47), and exposure to toluene, a toxic hydrocarbon (48). Changes also

* Corresponding author. Mailing address: University of California, Santa Barbara, Donald Bren School of Environmental Science & Management, Santa Barbara, CA 93106-5131. Phone: (805) 893-3195. Fax: (805) 893-7612. E-mail: holden@bren.ucsb.edu.

appear in response to toxic metals. For example, mixed-species Cd-exposed sulfate-reducing bacterial biofilms produced increased amounts of extracellular protein and carbohydrate (71). Chromium exposure also resulted in increased EPS production and changes in marine bacterial biofilm morphology under sulfate-reducing conditions (18). Also, an anaerobic bacterial consortia grown in a chemostat accumulated more EPS and cell lysis products upon exposure to Cr (3), but the association of Cr with either EPS or soluble microbial products was not quantified. While these examples suggest the possibility for similar effects in soil biofilms, EPS quantity and quality depend on growth conditions (56), which differ for saturated and unsaturated systems.

The purpose of this study was to quantify changes in the macromolecular composition of cellular and EPS fractions of unsaturated *Pseudomonas putida* mt-2 biofilms exposed to iron (Fe) and Cr and to relate such changes to Cr fates in the soil environment, where Cr is frequently bound to Fe oxides that are colonized by Cr- and Fe-reducing bacteria. Here, unsaturated biofilms refer to bacteria colonizing surfaces exposed to air and covered by only thin films of water (4, 26, 27, 53, 55), as would occur in vadose zones. We observed that Cr exposure increased EPS on a per-cell basis in membrane-cultivated unsaturated biofilms and that macromolecular chemistry varied with exposure to Cr. We also observed that Cr(VI) was completely reduced to Cr(III), which accumulated on cells and in EPS. Extraordinarily high amounts of extracellular DNA (eDNA) were also present, and additional studies were performed that confirmed an association between Cr(III) and eDNA which could contribute to Cr(III) biostabilization in vadose zones.

MATERIALS AND METHODS

Minerals and media. Hematite (Fe_2O_3) was synthesized according to standard methods (49), air dried, and autoclaved for 1 h. The synthesized hematite particles had a mean diameter of 32.2 μm and a mean specific surface area of 0.326 $\text{m}^2 \text{g}^{-1}$ as determined by a Malvern particle sizer (Malvern Instruments Ltd., Worcestershire, United Kingdom). To coat the hematite with dichromate, 0.20 g of hematite was equilibrated with 20 ml of a filter-sterilized (0.2 μm) solution (pH 7) of $\text{K}_2\text{Cr}_2\text{O}_7$ and NaNO_3 (0.65 and 4.25 g, respectively, per 1.0 liter H_2O) for 24 h in a shaking water bath (25°C, 100 rpm) following methods adapted from others (19, 24). All chemicals were reagent grade or better (Sigma Chemical, St. Louis, MO). The suspension was centrifuged (15,000 $\times g$, 30 min) and the supernatant discarded. The pellet was air dried and ground into a fine powder with a sterile, acid-washed mortar and pestle. By inductively coupled plasma atomic emission spectroscopy (ICP-AES) using a TJA High Resolution IRIS instrument (Thermo Electron Corporation, Waltham, MA) and sample incubation in 10% (vol/vol) aqua regia according to standard methods (61), 45.7 mg $\text{Cr}_2\text{O}_7^{2-}$ was bound to each gram of hematite.

Iron-deficient solid growth media contained 0.67 g glycerol-2-phosphate, 1.0 g NH_4Cl , 0.20 g $\text{MgSO}_4 \cdot 7\text{H}_2\text{O}$, 0.05 g $\text{CaCl}_2 \cdot 2\text{H}_2\text{O}$, 5.0 g succinic acid disodium salt anhydrous, and 4.19 g 3-(*N*-morpholino)propanesulfonic acid per 1.0 liter H_2O , plus a separate trace mineral stock solution (0.125 ml per liter of 0.05 g $\text{MnSO}_4 \cdot 7\text{H}_2\text{O}$, 0.065 g $\text{CoSO}_4 \cdot 7\text{H}_2\text{O}$, 0.023 g CuSO_4 , 0.033 g ZnSO_4 , and 0.024 g MoO_3 in 1.0 liter H_2O). Media were adjusted to pH 7 with 0.10 M NaOH and amended with 1.5% (wt/vol) Bacto agar (Difco, Fisher Scientific, Pittsburgh, PA) prior to sterilization by autoclaving. For aqueous media containing chromium, 0.0147 g $\text{K}_2\text{Cr}_2\text{O}_7$ (0.05 mM, 0.2- μm -filter-sterilized) was added prior to sterilization. Sterile medium containing the solidifying agent (75 ml) was dispensed into sterile, 150-mm-diameter, disposable plastic petri dishes.

Strain and biofilm cultivation. Biofilms were cultivated on membranes overlying solid medium, as described before (4, 53, 55). *P. putida* mt-2 (ATCC 33015) was maintained at -80°C in 70% Luria-Bertani broth plus 30% glycerol prior to biofilm cultivation. The inoculum was prepared by suspending one colony from solid (control) medium (30°C, 18 h) into 1 ml of sterile 0.9% NaCl solution.

Using medium that has the same chemical composition, this strain reaches late exponential phase after 18 h (30°C) in liquid culture (data not shown).

Four treatments were used: (i) control, (ii) Cr only (Cr), (iii) hematite only (Fe), and (iv) hematite plus Cr (Fe+Cr). For all treatments, Nuclepore polycarbonate membranes (47-mm diameter, 0.1- μm pore size, 6 μm thick; Whatman, Clifton, NJ) were cut into 1-cm squares, sterilized by immersion in 70% ethanol for 2 min, and then air dried briefly and transferred to the solid medium surface. Twenty membranes were spaced evenly onto each solid medium dish to ensure identical zones of nutrient depletion during growth (55). For the control treatment, membranes were placed directly onto the medium surface without additional metals. For the Fe treatment, hematite was first deposited onto the solid medium surface by dispensing 25- μl drops of a 30-g/liter suspension. Membranes were placed on top of the hematite after residual water associated with each drop had evaporated. Using these procedures, the hematite particles were well within the perimeter of the associated membrane. When appropriate, dichromate-coated hematite was deposited on the surface and membranes placed using similar techniques. The Cr treatment involved membranes placed onto solid medium containing 0.05 mM $\text{K}_2\text{Cr}_2\text{O}_7$. The treatments were independently triplicated by using three petri dishes for each treatment.

Membrane inoculation was adapted from the techniques of Steinberger and Holden (55). The liquid inoculum (2 μl) was dispensed onto the center of each membrane. Previously, this amount of *P. aeruginosa* PG201 inoculum contributed less than 1% of the final biofilm biomass (55). Petri dishes were sealed with parafilm and incubated (30°C, 72 h).

Biofilm harvesting and analysis. As with *P. aeruginosa* (55), biofilms grew radially and concentrically away from the point of inoculation. Harvesting for macromolecular analyses involved lifting six membranes off the solid medium surface with sterile forceps and combining a group of six membranes into a microcentrifuge tube containing 0.4 ml of 0.9% NaCl solution. This step was repeated three times for each petri dish, resulting in three samples from each dish. The remaining two biofilms from each dish were maintained intact at 4°C for staining prior to electron microscopy. Under identical conditions but separately, biofilms were cultivated for X-ray absorption near-edge spectroscopic (XANES) analysis (see below). Also under identical conditions but separately, biofilms were cultivated for the purposes of calibrating intracellular DNA to cell counts as described below. It was found through ICP-AES of uninoculated controls that no significant amount of deposited metal (Fe or Fe/Cr) was removed from the solid medium surface when membranes were harvested (data not shown).

After vortexing (10 s), membranes were discarded and the three suspensions for each petri dish were combined, resulting in a composite suspension from 18 replicate biofilms for each of the triplicated treatments. Cells and EPS were centrifugally separated (12,000 $\times g$ at 4°C for 30 min) as described before (55). The EPS-containing supernatants were decanted and stored at -20°C for further analysis. The cell pellets were resuspended in 2.5 ml of 1.0 M NaOH and lysed by heating (80°C, 1 h). The lysed cell suspension was then neutralized with 2.5 ml of 1.0 M HCl and stored (-20°C) until analysis. Total carbohydrates for both the EPS and cell fractions were quantified by the phenol-sulfuric acid method using glucose as the standard (17). Total protein was quantified using the Bradford method (6) with reagents from Bio-Rad (Hercules, CA). DNA was quantified by the Picogreen method (Molecular Probes, Eugene, OR) using calf thymus DNA as the standard. Glycosyl residues were derivatized, characterized, and quantified by gas chromatography/mass spectrometry (GC-MS) similarly to the method of York et al. (74) using a Hewlett-Packard 6890/5973 GC-MS instrument. Individual glycosyl residues were expressed on a mass-per-biofilm cell basis; their masses were also converted to glucose equivalents by applying the following formula:

$$\frac{\text{sugar mass}}{\text{mol wt sugar}} \times \frac{\text{moles C}}{\text{moles sugar}} \times \frac{\text{moles glucose}}{\text{moles C}} \times \text{mol wt glucose} \quad (1)$$

where mol wt is molecular weight.

In separate experiments using biofilms cultivated identically to the method described above, the amount of intracellular DNA (iDNA) (55) per cell was determined for each treatment as follows. Single biofilms were dispersed into 0.4 ml of 0.9% NaCl, and 0.1 ml of this suspension was reserved for iDNA analysis. Both the original sample and the subsample were centrifuged (12,000 $\times g$, 4°C, 30 min) and the supernatants discarded. The smaller pellet, used for counting intact cells, was suspended in 1.125 ml of 0.9% NaCl and 0.125 ml formaldehyde (37% aqueous solution; Sigma Chemical, St. Louis, MO). The larger pellet, used for quantifying iDNA, was lysed in 1 M NaOH (as above), neutralized using equivalent HCl, and stored at -20°C until DNA quantification by Picogreen fluorometry (as above). Within 24 h, aliquots of the intact cell suspension were

diluted 100 \times , and 150- μ l aliquots were combined with 2.85 ml of 0.9% NaCl and 0.6 μ l of SYBR Gold (Molecular Probes, Eugene, OR) in 3-ml, foil-wrapped tubes. The suspension was incubated at room temperature in the dark for 20 min and then filtered through an Anodisc filter (25-mm diameter, 0.2- μ m pore size; Whatman), which was then dried in the dark, mounted on a standard glass slide, and sealed with a coverslip. Cells were counted at a total magnification of \times 1,000 using an Eclipse E800 epifluorescence microscope (Nikon) and a green fluorescent protein filter set (Chroma, Rockingham, VT). Three replicate slides were prepared for each biofilm. Cells were counted in 10 separate fields per slide, and counts were averaged across the fields for each slide.

Biofilm staining and ESEM imaging. For each of the treatments, three biofilms from separate petri dishes were examined using environmental scanning electron microscopy (ESEM). Prior to imaging, the biofilms were removed from the solid growth medium using sterile forceps and stained with a combination of ruthenium red, glutaraldehyde, osmium tetroxide, and lysine according to previous methods (J. H. Priester, A. M. Horst, L. C. Van De Werfhorst, J. L. Saleta, L. A. K. Mertes, and P. A. Holden, submitted for publication). The biofilms were imaged on a Peltier stage (5 $^{\circ}$ C) in an FEI Co. XL30 FEG ESEM (Philips Electron Optics, Eindhoven, The Netherlands) operated in wet mode (\sim 4 Torr) at an accelerating voltage of 10 kV. Specimens were not conductively coated prior to imaging. A random-number-based scheme was used to select fields of view when acquiring biofilm images. Images (five per biofilm) used for assessing biofilm surface morphology and cell sizes were acquired at magnification \times 2,500; biofilm porosity was estimated from triplicate images taken at magnification \times 600.

Abiotic Cr desorption from hematite. One interest in this study was the possible involvement of biofilms in biotic desorption of Cr off of hematite-Fe. Such a process could be inferred only after accounting for the abiotic Cr desorption from hematite using solution chemistry identical to the biofilm culture conditions. Abiotic desorption of Cr from the Cr-coated hematite was tested by incubating (static, 30 $^{\circ}$ C) various amounts (3.8 mg, 8.8 mg, 16.3 mg, and 24.9 mg) of dichromate-coated hematite in 5 ml of sterile liquid growth medium. After 72 h, the samples were centrifuged to separate particulate metals from soluble constituents. Soluble metals were quantified using ICP-AES after preparing samples in 10% (vol/vol) aqua regia as before. The concentration was evaluated and principles of mass balance invoked to infer the amount of Cr liberated from hematite into solution.

XANES. Cr-K-edge XANES spectra were collected at the Stanford Synchrotron Radiation Laboratory beam line 11-2 under Stanford Positron Electron Asymmetric Ring 3 to determine the oxidation state of Cr. Triplicate samples for each treatment of biofilms, EPS, and cells were received overnight frozen and analyzed immediately. Biofilm samples were placed into the beam directly on the membrane support. Cell samples were filtered into a concentrated spot on a 0.2- μ m polycarbonate filter. EPS samples were measured in solution in a plastic sample holder using Kapton tape as the window material. Standards used for Cr oxidation state measurements were CrCl₃ for Cr(III) and K₂CrO₄ for Cr(VI). X-ray energy was selected using a Si(220) double-crystal monochromator, detuned 50% for harmonic rejection. Energy was calibrated by defining the first derivative peak of a Cr metal foil to be 5,989 eV. Samples were collected in fluorescence mode using a 30-element Ge array detector. The total incoming count rates from fluorescent photons were less than 10,000 s⁻¹ per element, which is well within the linear response range of the detector. Spectra were collected over the range from 5,980 to 6,025 eV using a step size of 0.5 eV through the edge. Individual scans typically took 5 min for completion to minimize radiation exposure to the sample. All spectra were averaged, background subtracted, and normalized using SIXPACK (69). In addition to analyzing the Cr oxidation state of biofilms from the various treatments, control biofilms were also studied for their potential to rapidly oxidize Cr(VI). The assessment was performed by transferring a 20- μ l drop of 2 mM Cr(VI) onto control biofilm membranes, followed by performing XANES after approximately 10 and 20 min of exposure. For comparison, a control biofilm was also subjected to 50 mM (Cr VI) to insure that no beam reduction artifacts were occurring.

Desorption of EPS-bound Cr. Dialysis studies were performed similarly to a method described previously (46), but in this case the purpose was to assess how much Cr was bound to EPS and whether Cr was specifically associated with extracellular DNA (eDNA). *P. putida* mt-2 biofilms (Cr treatment only) were inoculated and harvested, and EPS was separated from cells as described above. Enough biofilms were cultivated such that 20 biofilms were combined as 1 replicate in a treatment. All treatments were triplicated. The treatments included a control of undialyzed EPS in 0.9% NaCl, a test of dialyzed EPS in 0.9% NaCl, and dialyzed EPS in 0.9% NaCl treated with DNase I (Ambion, Austin, TX). An abiotic control for Cr transport through the dialysis tubing consisted of dialyzing 0.06 mg/ml Cr(III) [as Cr(NO₃)₃ · 9H₂O] in 0.9% NaCl. All treatments were

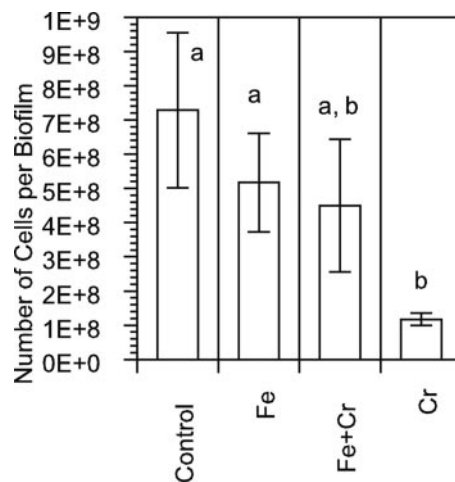


FIG. 1. Cellular yield of *Pseudomonas putida* mt-2 biofilms. Like letters indicate no significant difference ($P < 0.05$; $n = 3$).

dialyzed so that unbound Cr would equilibrate across the dialysis tube, resulting in significantly lower final concentrations in the tubing. Dialysis was performed in Spectra/Por 1, flat-width 10-mm membranes with a molecular weight cutoff of 6,000 to 8,000 (Fisher Scientific, Hampton, NH) using Nanopure water as the dialysis solution for 24 h. The water volume was approximately one liter and was changed after 12 h. Samples treated with DNase I were prepared by adding 100 μ l of the enzyme (in Tris-HCl) to each sample and incubating for 1 h at 37 $^{\circ}$ C. In this way, any Cr bound to eDNA would be liberated into solution upon DNA cleavage, and the relative role of eDNA in Cr binding could be inferred. Following dialysis, the contents of the dialysis tubes were sampled quantitatively into sterile tubes for drying. When the samples were completely dry, they were resuspended in 4 ml of 10% aqua regia and analyzed with ICP-AES for total chromium as before.

Data analysis. The content of macromolecules and metals in the EPS and cell fractions was normalized to the number of cells after determining the iDNA content on a per-cell basis for each treatment. The volumetric concentrations of metals in the biofilms were estimated by dividing the metal mass quantified for each biofilm by the biofilm volume. The biofilm volume (V_B) was calculated using the numbers of cells per biofilm (no. cells), the cellular volume (V_{cells}), and the biofilm porosity as follows:

$$V_B = \frac{V_{\text{cells}} \times \text{no. cells}}{1 - \text{porosity}} \quad (2)$$

Biofilm porosity was estimated from each of three \times 600-magnification ESEM images for each treatment in Photoshop 5.5 (Adobe, San Jose, CA) by dividing the area of space around cells by the total image area, assuming an equivalent projection into the third dimension (27).

Cellular dimensions were measured from ESEM images (\times 2,500) using Photoshop 5.5 for 10 randomly selected cells for each treatment. To quantify observed textural differences between biofilms, ESEM images were analyzed using the neighborhood variety statistic in Arcview GIS 3.2a (ESRI, Redlands, CA) as described before (Priester et al., submitted). The neighborhood variety statistic yields both maps of textural variety and histograms of pixel abundance versus variety. A rectangular 10-by-10 variety filter was used in Arcview. From the histogram data, a pixel-weighted mean variety statistic was calculated for each image. A relatively high mean variety results from texturally complex or rough samples, whereas a lower mean variety results when the specimen is smooth. Thus, the mean variety was used as a metric for comparing image textural differences between treatments which in turn resulted from differences in EPS abundance on the surfaces of biofilms.

All statistical analyses were performed using either SPSS 12.0.1 for Windows (SPSS Inc., Chicago, IL) or Microsoft Excel 2000 software. Means were compared by the Student *t* test. Where applicable, standard errors were propagated using accepted methods (58).

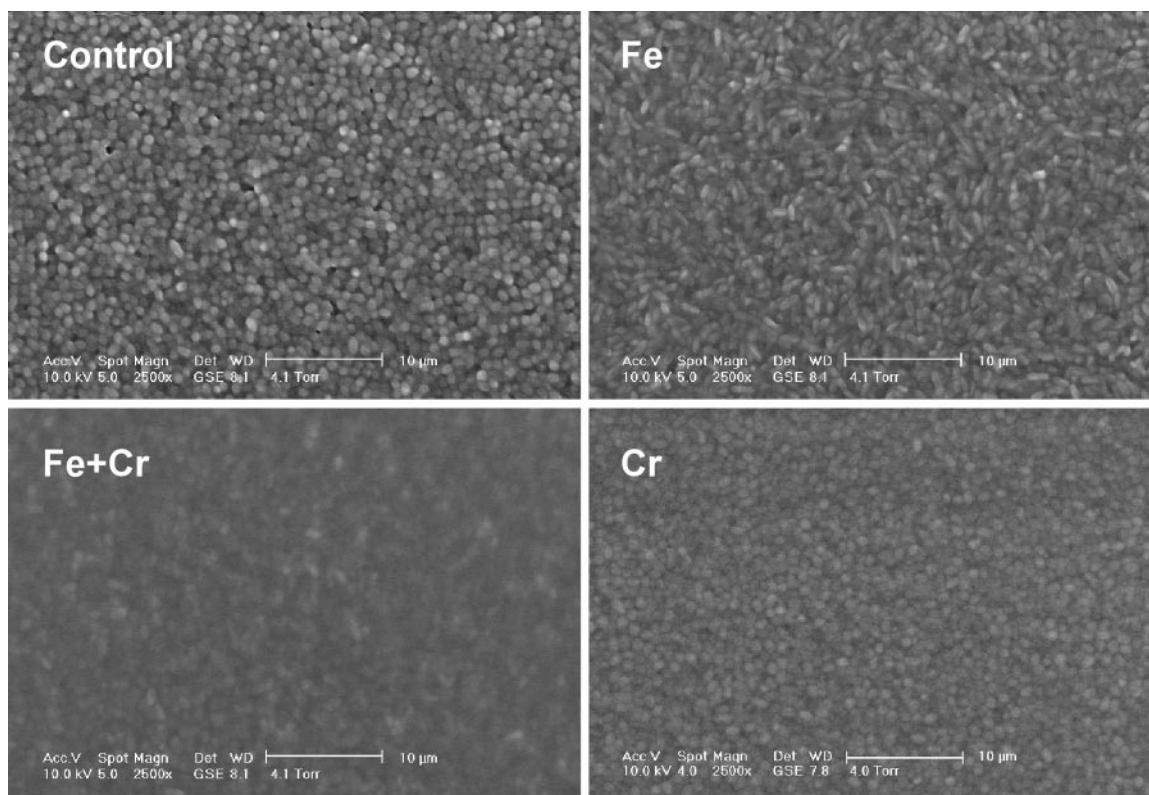


FIG. 2. Environmental scanning electron micrographs of *Pseudomonas putida* mt-2 unsaturated biofilms. Treatments are indicated in the figure and described in Materials and Methods. Scale bar = 10 μ m.

RESULTS

Yield. After 72 h, biofilm biomass was visibly greatest for the control treatment and least for the Cr and Fe+Cr treatments. The Fe treatment had intermediate biofilm growth. The total number of cells differed significantly only for the Cr treatment (Fig. 1), where cell counts were approximately one-third or less of those for the other treatments. In addition to total cell counts, iDNA is another proxy for biofilm yield (55). The control ($0.024 \pm 0.003 \mu\text{g}$) and Fe ($0.027 \pm 0.005 \mu\text{g}$) treatments yielded significantly greater amounts of iDNA per biofilm than the Cr ($0.0057 \pm 0.001 \mu\text{g}$) treatment. The control treatment also yielded significantly more iDNA than the Fe+Cr treatment ($0.013 \pm 0.002 \mu\text{g}$; $P = 0.01$). When compared to each other, the Fe+Cr and Fe treatments yielded similar amounts of iDNA per biofilm.

Other macromolecule contents in the biofilms also varied with treatment. The control biofilms contained significantly greater ($P = 0.03$) total (cellular plus EPS) protein ($0.14 \pm 0.006 \text{ mg}$) than those with the Cr treatment ($0.09 \pm 0.006 \text{ mg}$) and significantly more ($P = 0.01$) carbohydrate ($0.07 \pm 0.006 \text{ mg}$) than those with the Cr treatment ($0.02 \pm 0.006 \text{ mg}$). Total protein did not vary across the control, Fe ($0.14 \pm 0.006 \text{ mg}$), and Fe+Cr ($0.13 \pm 0.01 \text{ mg}$) treatments. The total carbohydrate in control biofilms was statistically greater ($P = 0.01$) than that in the Fe+Cr biofilm ($0.03 \pm 0.006 \text{ mg}$). The total carbohydrate for the Fe treatment ($0.06 \pm 0.01 \text{ mg}$) and the total protein for the Fe treatment did not differ from the respective macromolecular contents for the Fe+Cr treatment biofilms. Total DNA was highest for the Fe+Cr treatment

($0.20 \pm 0.006 \mu\text{g}$) in comparison to either the control ($0.11 \pm 0.01 \mu\text{g}$), the Fe ($0.15 \pm 0.006 \mu\text{g}$), or the Cr ($0.11 \pm 0.01 \mu\text{g}$) treatment.

Biofilm morphology. The biofilm diameters were between 5 and 10 mm, where the control treatment yielded the largest, and the Cr treatment the smallest, biofilms. The control treatment yielded thick, opaque biofilms with irregular edges. In contrast, the Cr and Fe+Cr biofilms were thin and semitransparent. Biofilms grown over hematite (Fe and Fe+Cr treatments) were pink. As indicated by the ESEM images (Fig. 2), individual cells in the control biofilms were easily distinguishable, while those in the biofilms exposed to the metals were not. Further, cells exposed to Fe were elongated (Table 1).

The mean variety of ESEM images, a measure of topographical irregularity on biofilm surfaces (J. H. Priester, A. M. Horst, L. C. Van De Werfhorst, J. L. Saleta, L. A. K. Mertes, and P. A. Holden, submitted for publication), was

TABLE 1. Average cellular dimensions^a

Treatment	Length ($\mu\text{m} \pm \text{SE}$)	Width ($\mu\text{m} \pm \text{SE}$)	Aspect ratio ($\pm \text{SE}$)
Control	1.13 ± 0.05 a	0.67 ± 0.04 d	1.72 ± 0.08 g
Fe	1.44 ± 0.07 c	0.51 ± 0.02 e	2.82 ± 0.13 i
Fe+Cr	1.34 ± 0.05 c	0.52 ± 0.03 f	2.59 ± 0.09 i
Cr	1.02 ± 0.03 b	0.73 ± 0.02 d	1.40 ± 0.05 h

^a Like letters in each column indicate differences that are not significant (t test, $P > 0.05$).

TABLE 2. Biofilm macromolecular composition normalized to biofilm cell count

Treatment	Amt of macromolecule (pg cell ⁻¹ ± SE) ^a					
	eDNA	iDNA × 10 ³	eProtein	iProtein	eCarbohydrate ^b	iCarbohydrate ^b
Control	0.014 ± 0.0046 ^a a	4.30 ± 0.82 c	11 ± 2.9 f	15 ± 2.3 h	5.8 ± 0.69 j, h	6.9 ± 1.7 l
Fe	0.013 ± 0.0024 ^a a	9.20 ± 0.45 d	9.3 ± 2.4 f	9.3 ± 0.58 h	3.8 ± 1.8 k	3.7 ± 0.58 l
Fe+Cr	0.15 ± 0.05 ^b b	4.30 ± 0.13 c, e	71 ± 17 g	18 ± 3.6 h	19 ± 9.8 j, k	4.8 ± 1.3 l
Cr	0.071 ± 0.02 ^b b	6.80 ± 0.87 e	58 ± 10 g	6.8 ± 0.58 i	13 ± 3.3 j	1.6 ± 0.58 m

^a The prefix “e” denotes the extracellular fraction; “i” as a prefix is for the intracellular fraction. Like letters in each column denote differences that are not significant (*t* test, *P* > 0.05).

^b Glucose equivalents, as per Materials and Methods.

highest for the control treatment (23.1 ± 0.7) and lowest for the Fe+Cr treatment (9.6 ± 0.2), indicating that the biofilms in the latter treatment were more smooth, possibly due to more EPS occupying divisions between cells. Images from the Fe and Cr treatments had intermediate values of mean variety (17.8 ± 0.5 and 16 ± 0.4, respectively). All differences in the mean variety across treatments were significant (*P* < 0.04).

Macromolecular composition. When macromolecular composition was expressed on a per-cell basis, total protein was highest in the Cr-exposed biofilms, but total biofilm carbohydrate did not vary with treatment (Table 2). Extracellular DNA and extracellular protein, when normalized to cell number, were significantly greatest for Cr- and Fe+Cr-exposed biofilms (Table 2). Intracellular DNA, expressed on a per-cell basis, was higher for the Fe+Cr treatment than for the Cr treatment (*P* = 0.02), but other differences were not significant (Table 2). Extracellular carbohydrate appeared to be greater for the Fe+Cr and Cr treatments (Table 2) than for the control and Fe treatments, but differences based on phenol-sulfuric acid assay data were not statistically significant. However, the quantities of EPS sugars determined by GC-MS, when converted to glucose-C equivalents (Table 3), were very similar to the amounts based on the phenol sulfuric acid method (Table 2), and by GC-MS, EPS sugars were significantly more abundant in Cr-exposed biofilms.

When normalized to iDNA, intracellular and extracellular macromolecules followed the same trend across treatments (not shown), i.e., that intracellular protein and carbohydrates were highest for the control treatment and lowest for the Cr treatment. Conversely, extracellular DNA, protein, and carbohydrates were highest for the Cr treatment and lowest for the control treatment.

EPS sugar composition. Nine EPS sugars were quantified by GC-MS. The seven commonly detected sugars and their amounts for each treatment are shown in Table 3, except for *N*-acetylglucosamine and glucuronic acid, which were only present in the Fe treatment at very low levels. For all sugars except xylose, the Fe+Cr and Cr treatments yielded the highest amounts on a per-cell basis, and except for glucose the amounts were similar across these two treatments. The Fe and control treatments yielded similar masses of sugars and only differed in EPS ribose abundances. Ribose and xylose abundances appeared invariant across treatments (Table 3).

Each sugar in Table 3 was converted to a glucose-equivalent mass as per equation 1. The total glucose equivalents by GC-MS of derivatized EPS were similar and were highest for the Fe+Cr and Cr treatments (Table 3). For all treatments, total glucose equivalents by GC-MS (Table 3) were quantitatively similar to glucose equivalents measured for EPS using the phenol sulfuric acid method (Table 2).

Metal distribution in biofilms. By ICP-AES of the EPS and cellular fractions of the biofilms, the Fe+Cr and Cr treatments accumulated a total of 0.16 ± 0.009 μg and 0.11 ± 0.003 μg of Cr per biofilm, respectively. Fe accumulation in the Fe+Cr and Fe treatments was 0.080 ± 0.02 μg and 0.040 ± 0.002 μg per biofilm, respectively. The total Cr content relative to iDNA did not vary between the Cr and Fe+Cr treatments and averaged 0.02 ± 0.003 μg/μg. Similarly, the total Cr concentration in the biofilm did not vary with treatment (*P* = 0.11) and averaged 0.47 ± 0.19 μg/mm³. The Cr content in the biofilms was approximately equally distributed between the cells and EPS. The total Fe content relative to iDNA did not vary across any of the four treatments and averaged 0.012 ± 0.008 μg/μg. Similarly, the total Fe concentration in the biofilm did not vary with

TABLE 3. Glycosyl residue content of EPS normalized to biofilm cell count

Sugar	Glycosyl residue content (pg cell ⁻¹ ± SE) with the following treatment ^a :			
	Control	Fe	Fe+Cr	Cr
Galactose	0.20 ± 0.036 a	0.16 ± 0.060 a	0.77 ± 0.21 b	0.29 ± 0.031 a, b
Glucose	1.58 ± 0.32 c	2.27 ± 1.57 c	8.17 ± 1.96 d	6.55 ± 1.00 d
<i>N</i> -Acetylglucosamine	0.024 ± 0.0043 e	0.057 ± 0.031 e, g	0.35 ± 0.11 f	0.12 ± 0.027 f, g
Mannose	0.42 ± 0.078 h	0.49 ± 0.14 h	2.28 ± 0.42 i	1.38 ± 0.25 i
Rhamnose	0.90 ± 0.19 j	0.91 ± 0.27 j	5.08 ± 0.74 k	3.56 ± 0.36 l
Ribose	ND ^c	0.093 ± 0.047 m	1.68 ± 1.06 m	0.19 ± 0.11 m
Xylose	0.0056 ± 0.0011 n	0.0098 ± 0.0046 n	0.018 ± 0.014 n	0.0072 ± 0.0038 n
Total glucose equivalents ^b	3.23 ± 0.65 o	4.10 ± 2.16 o	18.94 ± 4.60 p	11.88 ± 1.82 p

^a Like letters in each row indicate differences that are not significant (*t* test, *P* > 0.05).

^b Calculated as per Materials and Methods.

^c ND, not detected.

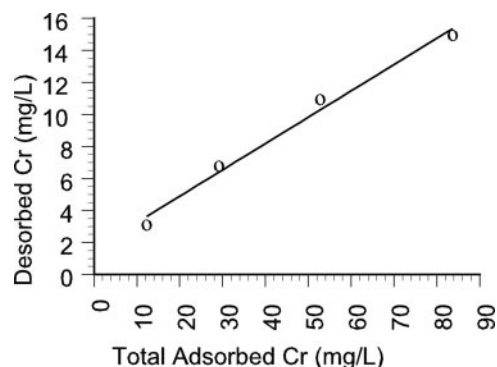


FIG. 3. Desorption isotherm for Cr mobilized from dichromate-coated hematite incubated in minimal medium at 30°C. The square of the linear regression coefficient (R^2) = 0.99.

treatment ($P > 0.07$) and averaged $0.11 \pm 0.04 \mu\text{g}/\text{mm}^3$. However, in all treatments, Fe was associated only with the cells.

Based on the difference between Cr initially adsorbed to the hematite and the final Cr concentration in the Fe+Cr-treated biofilm, approximately 1% of the Cr on the Cr-treated hematite was mobilized into the biofilm. However, little of this mobilization into biofilm, if any, can be attributed to cellular activity, since the mineral medium readily liberated Cr from the hematite (Fig. 3). Also, using the desorption isotherm in Fig. 3 and assuming conservation of mass, calculations showed that approximately 0.20 mg of Cr would have been mobilized into the solid mineral medium by simple (abiotic) desorption and diffusion alone. This would have resulted in an equilibrium concentration of Cr in the solid medium associated with the Cr-coated hematite of 0.05 mM, which was equivalent to the Cr concentration in the solid medium for the Cr-only treatment.

Cr oxidation state. Cr oxidation state in the biofilm and biofilm components was assessed by XANES. The spectra for Cr standards show the expected shift of the main absorption edge to higher energies with increasing oxidation state (Fig. 4). In addition, the spectra for Cr(VI) are characterized by a very intense $1s \rightarrow 3d$ pre-edge transition at $\sim 5,993$ eV, which is almost insignificant in Cr(III). These differences in XANES

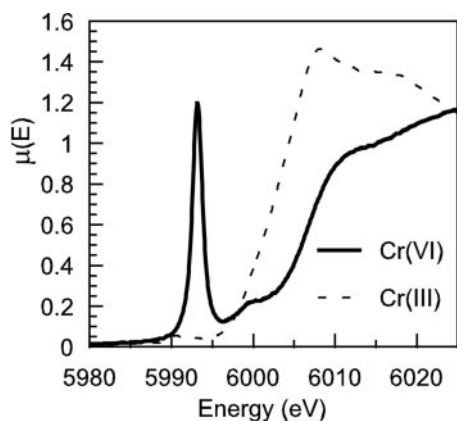


FIG. 4. Cr K-edge XANES spectra for Cr(III) and Cr(VI) compounds used as standards.

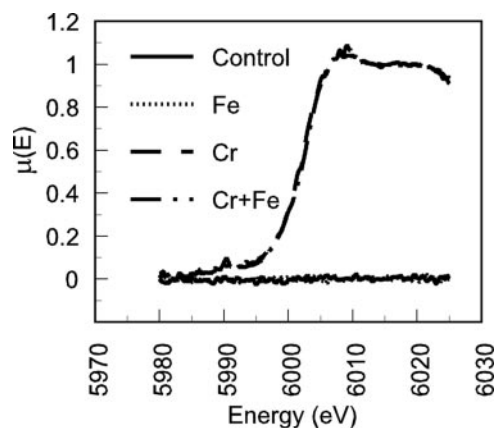


FIG. 5. Cr K-edge XANES spectra for biofilm samples under the four experimental treatments. The lower coincident lines trace the control and Fe data; the upper coincident lines trace the two Cr treatments.

spectra allow for the determination of the oxidation states of Cr in the samples.

Figure 5 shows the spectra obtained for biofilms produced under the four growth conditions. Biofilms where Cr was not added did not show the presence of any Cr in the sample. The Cr-added and Fe+Cr biofilms both showed that all of the Cr(VI) added to the biofilms had been reduced to Cr(III). If Cr(VI) was present in the samples, it was below the detection limits, i.e., ca. 3% of the total Cr. Samples of separated cells and EPS also showed that all of the Cr in the specific portions of the biofilm had been reduced to Cr(III) (data not shown).

Cr(VI) was added to a control biofilm (2 mM) before XANES measurement to examine the ability of the biofilm to rapidly reduce Cr. Measurements after 10 and 20 min of contact (Fig. 6) show that the reduction of Cr(VI) to Cr(III) is very rapid and is nearly complete after 20 min for these biofilms when not previously exposed to Cr. When control biofilms were exposed briefly to 50 mM Cr(VI), there was no change in the spectra,

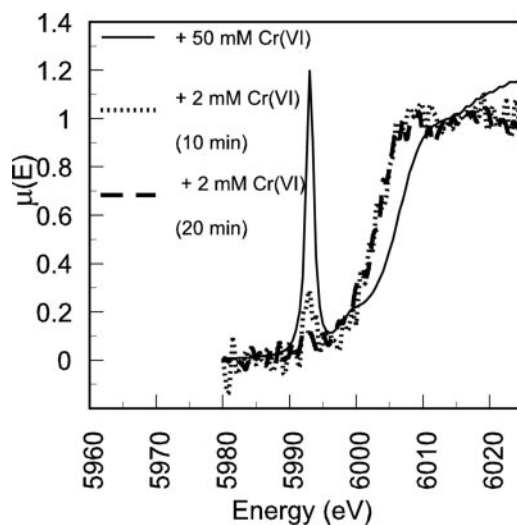


FIG. 6. Cr K-edge XANES spectra for control biofilms exposed either to 50 mM Cr(VI) briefly or to 2 mM Cr(VI) over a time course.

suggesting that exposure to the X-ray beam did not cause artifactual reduction of Cr(III) (Fig. 6).

Cr desorption from biofilm EPS. To study desorption of Cr from EPS, biofilms cultured with Cr only were harvested, the EPS dialyzed against deionized water, and the Cr content was measured in the dialyzed EPS. As per Methods, we treated one EPS sample with DNase I, because we hypothesized that eDNA was sorbing Cr(III) and that breakdown of DNA would release sorbed Cr. Three controls were studied for comparison: one of undialyzed EPS, another of dialyzed but untreated (no DNase) EPS, and another, strictly abiotic, control to verify that Cr would readily pass the dialysis membrane. Cr(III) readily passed through the dialysis membrane in that 99.6% of the chromium in Cr-salt samples (no EPS) was removed during dialysis. The total chromium content of the untreated (dialyzed and undialyzed) EPS samples did not differ significantly (*t* test, $P = 0.22$) and averaged $0.08 \pm 0.05 \mu\text{g/ml}$, suggesting that Cr did not desorb from the EPS during routine dialysis. However, for the EPS samples treated with DNase I, chromium was not detected in the EPS sample following dialysis, which demonstrated that Cr was sorbed to eDNA in the EPS.

DISCUSSION

While Cr(VI) is known to reduce biotically to Cr(III) in the vadose zone (42), the biotic factors controlling the fate of reduced Cr in the vadose zone are not well understood. In this study, unsaturated *P. putida* mt-2 biofilms completely reduced Cr(VI) to Cr(III) and concentrated Cr by nearly 180-fold relative to their external environment. Not surprisingly, Cr(III) was associated with both the cells and EPS. However, surprisingly, eDNA and extracellular Cr(III) were found to be sorbed to one another. Sorption of Cr(III) to eDNA, the latter of which is now known to be common in unsaturated biofilms (54, 55), accounted for high amounts of each in the extracellular matrix of these biofilms and may be a newly identified mode for biotic Cr(III) stabilization in the vadose zone.

Many bacteria can reduce chromate under aerobic and anaerobic conditions (8) where the responsible enzymes are constitutive chromate reductases (30, 32, 44). Accumulation of Cr at rates of 40.7 mg/liter (0.78 mM) total Cr per day in a mixed-species biofilm containing *Pseudomonas* spp. has been reported (11). Rapid chromate reduction to Cr(III) has been observed for soluble chromate reductases isolated from *P. putida* MK1 (44), *P. putida* PRS2000 (30), *Pseudomonas ambigua* (28), *Arthrobacter* spp., and *Bacillus* spp. (7, 40). Some of these reductases are NADH or NADPH dependent (7, 28, 30, 44), and some, for example, from a soil pseudomonad (39), are not. For the latter isolate, the reductase originated in the cytoplasm, left cells by lysis or secretion, and reduced Cr(VI) extracellularly, leaving Cr deposits on the cell envelope and bound to EPS and in solution (39). Cr(III) was both cellular and extracellular in our study, and thus, it is possible that cell lysis released constitutive reductases that catalyzed the extracellular reduction of Cr(VI) to Cr(III). Regardless of where Cr(VI) occurred, our previously frozen, control biofilms rapidly reduced Cr(VI) to Cr(III) (Fig. 6), which supports that the process was constitutive.

The native ability to reduce Cr(VI) to Cr(III) is important given that Cr(VI) is toxic to bacteria. In the present study, the

Cr(VI) concentration in the Cr-only treatment (0.05 mM as $\text{K}_2\text{Cr}_2\text{O}_7$ or 0.1 mM as Cr) and the amount of potassium dichromate-coated hematite in the Fe+Cr treatment were both selected to avoid severe toxicity based on prior reports. For example, toxicity thresholds reported for one planktonic *Pseudomonas* sp. were 4.3 mg liter⁻¹ (0.083 mM) in succinate and 8.8 mg liter⁻¹ (0.17 mM) in Luria-Bertani broth (33). The toxicity threshold for *P. aeruginosa* A2Chr was between 10 mg/liter (0.19 mM) and 40 mg/liter (0.77 mM) (22, 23) and for another *Pseudomonas* sp. was 10.4 mg/liter (0.2 mM) Cr(VI) (64). These studies were for planktonic cultures, but toxicity thresholds were similar for biofilm-cultivated and planktonic cells when investigated across several bacterial species, including *P. aeruginosa* (25). In our study, cells were obviously stressed, as indicated by the lower yield, lower protein and carbohydrate levels per cell, and increased extracellular macromolecules in biofilms exposed to Cr.

Many different environmental stresses have been previously reported to effect an increased production of extracellular carbohydrates in biofilms. Desiccation resulted in increased polysaccharide production by a *Pseudomonas* sp. (47). Trivalent chromium resulted in a nearly 82% increase in extracellular carbohydrate in sulfate-reducing bacterial biofilms (18). Mixed-species sulfate-reducing bacterial biofilms also exhibited an increase in extracellular carbohydrates when exposed to cadmium, possibly as a result of metal binding polymer production (71). *P. putida* biofilms exposed to toluene showed a significant increase in extracellular carbohydrate, and the composition shifted towards increasing carboxylic groups (48). We also observed changes in the carbohydrate composition of *P. putida* biofilms exposed to Cr. All of the sugars shown in Table 3 were present in significantly greater amounts in the Cr and Fe+Cr treatments than in the control treatment. The greatest increases were for glucose, *N*-acetylglucosamine, mannose, and rhamnose. As for *P. aeruginosa* (55), glucose and rhamnose were the predominant biofilm saccharides. For *P. ambigua*, glucose protected the chromate reductase enzyme from inactivation (28), which may be a role for EPS glucose in this study. The EPS glycosyl changes could also facilitate cation binding, as was proposed by Schmitt et al. (48), and could lead to the retention of soluble Cr(III) as an organo-complex (46). On the other hand, Cr(III) may bind to many macromolecules besides polysaccharides (46). Our work suggests a particularly important role for eDNA.

EPS was clearly enriched in eDNA relative to intracellular concentrations, which suggests that although DNA was liberated into the EPS, it was also stabilized. In this study, eDNA relative to cellular DNA was high for all treatments but exceptionally so for biofilms exposed to Cr (e.g., 10-fold higher in the Cr-only treatment). Cellular DNA was conserved across treatments and matched expected femtogram levels for laboratory and environmental bacteria (45), suggesting that the eDNA levels reported here were not methodological artifacts. DNA in bacterial EPS has been reported previously for saturated (57) and unsaturated (54, 55) biofilms with a suggested release mechanism of cell lysis. DNA can also be transported outside the cell by vesicles and is necessary for early *P. aeruginosa* biofilm growth (70). However, we believe that enhanced EPS macromolecules in our study were probably due to accelerated cell lysis, as reported previously for an anaerobic consortium exposed to chromium (3). As evidence, we observed that the

proportions of intracellular proteins and carbohydrates were preserved extracellularly.

The extracellular accumulation of both DNA and Cr(III) implies an association between these two molecules in the biofilm. Cr(III) accumulated in our biofilms to approximately 470 mg liter⁻¹ (9 mM), which was remarkably higher than either the initial 0.05 mM level of Cr(VI) in the Cr-only solid medium or the calculated final 0.05 mM level of Cr in the solid medium for the Fe+Cr treatment. As above, DNA also accumulated in the biofilms exposed to Cr. Cr(III) is known to bind to DNA in eukaryotic cells (10, 15, 21, 51, 52, 65, 73). Recently, a specific role for eDNA in saturated biofilms was suggested (70). Thus far, only the presence and abundance of eDNA in unsaturated *P. aeruginosa* biofilms have been reported (54, 55). However, based on the cooccurrences of high Cr and DNA concentrations in the EPS and the complete release of Cr from DNase I-treated EPS, our work provides sound evidence for *P. putida* eDNA binding Cr(III). We hypothesize that this could be a newly discovered mechanism by which Cr(III) is stabilized in vadose zone bacterial biofilms.

One goal of this study that merits further study is the possible role of biofilm EPS in liberating Fe-bound Cr from soil minerals. Because the succinate-based growth medium used here facilitated ample abiotic desorption of Cr(VI) from hematite, we could not ascribe Cr desorption from hematite to any biotic mechanism. We can conclude, however, that providing Fe(III) in the form of hematite compensated somewhat for Cr toxicity, as indicated by higher yield and internal macromolecules. We also observed that cells cultivated over hematite were elongated, leading us to conclude that, similarly to what was observed by Steinberger et al. (53), the iron mineral surface effectively caused a diffusional constraint on nutrient resupply, which is expected in unsaturated porous media. Finally, we can conclude that Cr was dissociated from iron in the EPS and that Cr accumulated in eDNA, perhaps by one of the already-established binding processes central to Cr-mediated mutagenesis. Future studies, perhaps using alternative solution chemistries that exclude Cr-binding ligands from the growth media, would be needed to determine if eDNA plays a role in mobilizing Cr(VI) into the biofilm for subsequent reduction.

ACKNOWLEDGMENTS

This work was supported by the LANL-CARE, the U.S. DOE NABIR, the U.S. EPA STAR, and the NSF MRI and Observatories programs. Portions of this research were carried out at the Stanford Synchrotron Radiation Laboratory, a national user facility operated by Stanford University on behalf of the U.S. Department of Energy, Office of Basic Energy Sciences. The SSRL Environmental Remediation Science Program is supported by the Department of Energy, Office of Biological and Environmental Research.

ESEM was performed in MEIAF (<http://www.bren.ucsb.edu/facilities/MEIAF/>) at UCSB by Jose Saleta. Laurie Van De Werfhorst (UCSB) performed the GC-MS quantification of glycosyl residues.

REFERENCES

- Alvarez, A. H., R. Moreno-Sanchez, and C. Cervantes. 1999. Chromate efflux by means of the ChrA chromate resistance protein from *Pseudomonas aeruginosa*. *J. Bacteriol.* **181**:7398–7400.
- Andreoni, V., M. Colombo, A. Colombo, A. Vecchio, and C. Finoli. 2003. Cadmium and zinc removal by growing cells of *Pseudomonas putida* strain B14 isolated from a metal-impacted soil. *Ann. Microbiol.* **53**:135–148.
- Aquino, S. F., and D. C. Stuckey. 2004. Soluble microbial products formation in anaerobic chemostats in the presence of toxic compounds. *Water Res.* **38**:255–266.
- Auerbach, I. D., C. Sorensen, H. G. Hansma, and P. A. Holden. 2000. Physical morphology and surface properties of unsaturated *Pseudomonas putida* biofilms. *J. Bacteriol.* **182**:3809–3815.
- Blenkinsopp, S. A., and J. W. Costerton. 1991. Understanding bacterial biofilms. *Trends Biotechnol.* **9**:138–143.
- Bradford, M. M. 1976. A rapid and sensitive method for the quantitation of microgram quantities of protein utilizing the principle of protein-dye binding. *Anal. Biochem.* **72**:248–254.
- Camargo, F. A. O., B. C. Okeke, F. M. Bento, and W. T. Frankenberger. 2003. In vitro reduction of hexavalent chromium by a cell-free extract of *Bacillus* sp ES 29 stimulated by Cu²⁺. *Appl. Microbiol. Biotechnol.* **62**:569–573.
- Cervantes, C. 1991. Bacterial interactions with chromate. *Antonie Leeuwenhoek* **59**:229–233.
- Chen, J. H., L. W. Lion, W. C. Ghiorse, and M. L. Shuler. 1995. Mobilization of adsorbed cadmium and lead in aquifer material by bacterial extracellular polymers. *Water Res.* **29**:421–430.
- Cohen, M. D., B. Kargacin, C. B. Klein, and M. Costa. 1993. Mechanisms of chromium carcinogenicity and toxicity. *Crit. Rev. Toxicol.* **23**:255–281.
- Coleman, R. N., and J. H. Paran. 1991. Biofilm concentration of chromium. *Environ. Technol.* **12**:1079–1093.
- Cook, K. R. 2000. In situ treatment of soil and groundwater contaminated with chromium: technical resource guide, p. 84. PA 625-R-00-005, vol. EPA/625/R-00/005. NRMRL Center for Environmental Research Information, Office of Research and Development (ed.), U.S. Environmental Protection Agency, Washington, D.C.
- Costerton, J. W., R. T. Irvin, and K. J. Cheng. 1981. The bacterial glycocalyx in nature and disease. *Annu. Rev. Microbiol.* **35**:299–324.
- Davey, M. E., and G. A. O'Toole. 2000. Microbial biofilms: from ecology to molecular genetics. *Microbiol. Mol. Biol. Rev.* **64**:847–867.
- Deflora, S., M. Bagnasco, D. Serra, and P. Zanacchi. 1990. Genotoxicity of chromium compounds—a review. *Mutat. Res.* **238**:99–172.
- Ding, M., and X. L. Shi. 2002. Molecular mechanisms of Cr(VI)-induced carcinogenesis. *Mol. Cell. Biochem.* **234**:293–300.
- Dubois, M., K. A. Gilles, J. K. Hamilton, P. A. Rebers, and F. Smith. 1956. Colorimetric method for determination of sugars and related substances. *Anal. Chem.* **28**:350–356.
- Fang, H. H. P., L. C. Xu, and K. Y. Chan. 2002. Effects of toxic metals and chemicals on biofilm and biocorrosion. *Water Res.* **36**:4709–4716.
- Fendorf, S., M. J. Eick, P. Grossl, and D. L. Sparks. 1997. Arsenate and chromate retention mechanisms on goethite. 1. Surface structure. *Environ. Sci. Technol.* **31**:315–320.
- Fendorf, S., B. W. Wielinga, and C. M. Hansel. 2000. Chromium transformations in natural environments: the role of biological and abiological processes in chromium(VI) reduction. *Int. Geol. Rev.* **42**:691–701.
- Flores, A., and J. M. Perez. 1999. Cytotoxicity, apoptosis, and in vitro DNA damage induced by potassium chromate. *Toxicol. Appl. Pharm.* **161**:75–81.
- Ganguli, A., and A. K. Tripathi. 2002. Bioremediation of toxic chromium from electroplating effluent by chromate-reducing *Pseudomonas aeruginosa* A2Chr in two bioreactors. *Appl. Microbiol. Biotechnol.* **58**:416–420.
- Ganguli, A., and A. K. Tripathi. 1999. Survival and chromate reducing ability of *Pseudomonas aeruginosa* in industrial effluents. *Lett. Appl. Microbiol.* **28**:76–80.
- Grossl, P. R., M. Eick, D. L. Sparks, S. Goldberg, and C. C. Ainsworth. 1997. Arsenate and chromate retention mechanisms on goethite. 2. Kinetic evaluation using a pressure-jump relaxation technique. *Environ. Sci. Technol.* **31**:321–326.
- Harrison, J. J., H. Ceri, C. A. Stremick, and R. J. Turner. 2004. Biofilm susceptibility to metal toxicity. *Environ. Microbiol.* **6**:1220–1227.
- Holden, P. A. 2001. Biofilms in unsaturated environments. *Methods Enzymol.* **337**:125–143.
- Holden, P. A., J. R. Hunt, and M. K. Firestone. 1997. Toluene diffusion and reaction in unsaturated *Pseudomonas putida* mt-2 biofilms. *Biotechnol. Bioeng.* **56**:656–670.
- Horitsu, H., S. Futo, Y. Miyazawa, S. Ogai, and K. Kawai. 1987. Enzymatic reduction of hexavalent chromium by hexavalent chromium tolerant *Pseudomonas ambigua* G-1. *Agric. Biol. Chem. (Tokyo)* **51**:2417–2420.
- Hunt, A. P., J. Hamilton-Taylor, and J. D. Parry. 2001. Trace metal interactions with epilithic biofilms in small acidic mountain streams. *Arch. Fur. Hydrobiol.* **153**:155–176.
- Ishibashi, Y., C. Cervantes, and S. Silver. 1990. Chromium reduction in *Pseudomonas putida*. *Appl. Environ. Microb.* **56**:2268–2270.
- Iyer, A., K. Mody, and B. Jha. 2004. Accumulation of hexavalent chromium by an exopolysaccharide producing marine *Enterobacter cloacae*. *Mar. Pollut. Bull.* **49**:974–977.
- Kamaludeen, S. P. B., M. Megharaj, A. L. Juhász, N. Sethunathan, and R. Naidu. 2003. Chromium-microorganism interactions in soils: remediation implications, p. 93–164. *Rev. Environ. Contam. Toxicol.* **178**:93–164.
- Khare, S., A. Ganguli, and A. K. Tripathi. 1997. Responses of *Pseudomonas aeruginosa* to chromium stress. *Eur. J. Soil Biol.* **33**:153–158.
- Langley, S., and T. J. Beveridge. 1999. Metal binding by *Pseudomonas aerugi-*

- nosa* PAO1 is influenced by growth of the cells as a biofilm. *Can. J. Microbiol.* **45**:616–622.
35. **Ledin, M.** 2000. Accumulation of metals by microorganisms—processes and importance for soil systems. *Earth-Sci. Rev.* **51**:1–31.
 36. **Lloyd, J. R., and D. R. Lovley.** 2001. Microbial detoxification of metals and radionuclides. *Curr. Opin. Biotechnol.* **12**:248–253.
 37. **Long, J. C. S.** 2000. Research needs in subsurface science. National Academy Press, Washington, D.C.
 38. **Losi, M. E., C. Amrhein, and W. T. Frankenberger.** 1994. Environmental biochemistry of chromium. *Rev. Environ. Contam. Toxicol.* **136**:91–121.
 39. **McLean, J., and T. J. Beveridge.** 2001. Chromate reduction by a pseudomonad isolated from a site contaminated with chromated copper arsenate. *Appl. Environ. Microbiol.* **67**:1076–1084.
 40. **Megharaj, M., S. Avudainayagam, and R. Naidu.** 2003. Toxicity of hexavalent chromium and its reduction by bacteria isolated from soil contaminated with tannery waste. *Curr. Microbiol.* **47**:51–54.
 41. **Mullen, M. D., D. C. Wolf, F. G. Ferris, T. J. Beveridge, C. A. Flemming, and G. W. Bailey.** 1989. Bacterial sorption of heavy metals. *Appl. Environ. Microbiol.* **55**:3143–3149.
 42. **Oliver, D. S., F. J. Brockman, R. S. Bowman, and T. L. Kieft.** 2003. Microbial reduction of hexavalent chromium under vadose zone conditions. *J. Environ. Qual.* **32**:317–324.
 43. **Palmer, C. D., and P. R. Wittbrodt.** 1991. Processes affecting the remediation of chromium-contaminated sites. *Environ. Health Persp.* **92**:25–40.
 44. **Park, C. H., M. Keyhan, B. Wieling, S. Fendorf, and A. Matin.** 2000. Purification to homogeneity and characterization of a novel *Pseudomonas putida* chromate reductase. *Appl. Environ. Microbiol.* **66**:1788–1795.
 45. **Paul, E. A., and F. E. Clark.** 1996. Soil microbiology and biochemistry, 2nd ed. Academic Press, San Diego, Calif.
 46. **Puzon, G. J., A. G. Roberts, D. M. Kramer, and L. Y. Xun.** 2005. Formation of soluble organo-chromium(III) complexes after chromate reduction in the presence of cellular organics. *Environ. Sci. Technol.* **39**:2811–2817.
 47. **Roberson, E. B., and M. K. Firestone.** 1992. Relationship between desiccation and exopolysaccharide production in a soil *Pseudomonas* sp. *Appl. Environ. Microb.* **58**:1284–1291.
 48. **Schmitt, J., D. Nivens, D. C. White, and H. C. Flemming.** 1995. Changes of biofilm properties in response to sorbed substances—an FTIR-ATR study. *Water Sci. Technol.* **32**:149–155.
 49. **Schwertmann, U., and R. M. Cornell.** 2000. Iron oxides in the laboratory: preparation and characterization, 2nd ed. Wiley-VCH, New York, N.Y.
 50. **Singh, P., and S. S. Cameotra.** 2004. Enhancement of metal bioremediation by use of microbial surfactants. *Biochem. Biophys. Res. Commun.* **319**:291–297.
 51. **Snow, E. T.** 1992. Metal carcinogenesis—mechanistic implications. *Pharmacol. Therapeut.* **53**:31–65.
 52. **Stearns, D. M., L. J. Kennedy, K. D. Courtney, P. H. Giangrande, L. S. Pihfeffer, and K. E. Wetterhahn.** 1995. Reduction of chromium(VI) by ascorbate leads to chromium DNA-binding and DNA strand breaks in-vitro. *Biochemistry* **34**:910–919.
 53. **Steinberger, R. E., A. R. Allen, H. G. Hansma, and P. A. Holden.** 2002. Elongation correlates with nutrient deprivation in *Pseudomonas aeruginosa* unsaturated biofilms. *Microb. Ecol.* **43**:416–423.
 54. **Steinberger, R. E., and P. A. Holden.** 2005. Extracellular DNA in single and multiple-species unsaturated biofilms. *Appl. Environ. Microbiol.* **71**:5404–5410.
 55. **Steinberger, R. E., and P. A. Holden.** 2004. Macromolecular composition of unsaturated *Pseudomonas aeruginosa* biofilms with time and carbon source. *Biofilms* **1**:37–47.
 56. **Sutherland, I. W.** 2001. Biofilm exopolysaccharides: a strong and sticky framework. *Microbiology* **147**:3–9.
 57. **Sutherland, I. W.** 2001. The biofilm matrix—an immobilized but dynamic microbial environment. *Trends Microbiol.* **9**:222–227.
 58. **Taylor, J. R.** 1997. An introduction to error analysis: the study of uncertainties in physical measurements, 2nd ed. University Science Books, Sausalito, Calif.
 59. **Teitzel, G. M., and M. R. Parsek.** 2003. Heavy metal resistance of biofilm and planktonic *Pseudomonas aeruginosa*. *Appl. Environ. Microbiol.* **69**:2313–2320.
 60. **Unz, R. F., and K. L. Shuttleworth.** 1996. Microbial mobilization and immobilization of heavy metals. *Curr. Opin. Biotechnol.* **7**:307–310.
 61. **U.S. Environmental Protection Agency.** 1991. Methods for the determination of metals in environmental samples. EPA/600/4-91/010. U.S. Environmental Protection Agency, Washington, D.C.
 62. **Vesper, S. J., R. DonovanBrand, K. P. Paris, S. R. AlAbed, J. A. Ryan, and W. J. DavisHoover.** 1996. Microbial removal of lead from solid media and soil. *Water Air Soil Pollut.* **86**:207–219.
 63. **Vincze, G., J. Vallner, A. Balogh, and F. Kiss.** 2000. Altered elemental composition of the cell wall of a *Pseudomonas* strain having inducible tolerance mechanism to chromium(VI). *Bull. Environ. Contam. Toxicol.* **65**:772–779.
 64. **Viti, C., A. Pace, and L. Giovannetti.** 2003. Characterization of Cr(VI)-resistant bacteria isolated from chromium-contaminated soil by tannery activity. *Curr. Microbiol.* **46**:1–5.
 65. **Voitkun, V., A. Zhitkovich, and M. Costa.** 1998. Cr(III)-mediated crosslinks of glutathione or amino acids to the DNA phosphate backbone are mutagenic in human cells. *Nucleic Acids Res.* **26**:2024–2030.
 66. **Volesky, B., and Z. R. Holan.** 1995. Biosorption of heavy-metals. *Biotechnol. Progr.* **11**:235–250.
 67. **Wang, Y.-T.** 2000. Microbial reduction of chromate, p. 225–235. *In* D. R. Lovely (ed.), *Environmental microbe-metal interactions*. American Society for Microbiology, Washington, D.C.
 68. **Ward, C. H.** 1999. Groundwater soil & cleanup. National Academy Press, Washington, D.C.
 69. **Webb, S. M.** 2005. Sixpack: a graphical user interface for XAS analysis using IFEFFIT. *Phys. Scripta T* **115**:1011–1014.
 70. **Whitchurch, C. B., T. Tolker-Nielsen, P. C. Ragas, and J. S. Mattick.** 2002. Extracellular DNA required for bacterial biofilm formation. *Science* **295**:1487.
 71. **White, C., and G. M. Gadd.** 1998. Accumulation and effects of cadmium on sulphate-reducing bacterial biofilms. *Microbiology* **144**:1407–1415.
 72. **Wolfaardt, G. M., J. R. Lawrence, J. V. Headley, R. D. Robarts, and D. E. Caldwell.** 1994. Microbial exopolymers provide a mechanism for bioaccumulation of contaminants. *Microb. Ecol.* **27**:279–291.
 73. **Xu, J., G. J. Bubleby, B. Detrick, L. J. Blankenship, and S. R. Patierno.** 1996. Chromium(VI) treatment of normal human lung cells results in guanine-specific DNA polymerase arrest, DNA-DNA cross-links and S-phase blockade of cell cycle. *Carcinogenesis* **17**:1511–1517.
 74. **York, W. S., A. G. Darvill, M. McNeill, T. T. Stevenson, and P. Albersheim.** 1986. Isolation and characterization of cell walls and cell wall components. *Methods Enzymol.* **118**:3–40.